



Published in final edited form as:

Oncogene. 2011 December 15; 30(50): 4990–4998. doi:10.1038/onc.2011.205.

THE RON RECEPTOR PROMOTES PROSTATE TUMOR GROWTH IN THE TRAMP MOUSE MODEL

Megan N. Thobe¹, Jerilyn K. Gray¹, Devikala Gurusamy¹, Andrew M. Paluch¹, Purnima K. Wagh¹, Peterson Pathrose¹, Alex B. Lentsch², and Susan E. Waltz^{1,3,*}

¹Department of Cancer and Cell Biology University of Cincinnati College of Medicine, Cincinnati, OH 45267-0521

²Department of Surgery, University of Cincinnati College of Medicine, Cincinnati, OH 45267-0521

³Cincinnati Veterans Affairs Medical Center, Cincinnati, OH 45220

Abstract

The Ron receptor tyrosine kinase is overexpressed in many cancers, including prostate cancer. In order to examine the significance of Ron in prostate cancer *in vivo*, we utilized a genetically engineered mouse model, referred to as TRAMP mice, that is predisposed to develop prostate tumors. In this model, we demonstrate that prostate tumors from 30-week-old TRAMP mice have increased Ron expression compared to age-matched wild-type prostates. Based on the upregulation of Ron in human prostate cancers and in this murine model of prostate tumorigenesis, we hypothesized that this receptor plays a functional role in the development of prostate tumors. To test this hypothesis, we crossed TRAMP mice with mice that are deficient in Ron signaling (TK^{-/-}). Interestingly, TK^{-/-} TRAMP⁺ mice show a significant decrease in prostate tumor mass relative to TRAMP mice containing functional Ron. Moreover, TK^{-/-} TRAMP⁺ prostate tumors exhibited decreased tumor vascularization relative to TK^{+/+} TRAMP⁺ prostate tumors, which correlated with reduced levels of the angiogenic molecules VEGF and CXCL2. While Ron loss did not alter tumor cell proliferation, a significant decrease in cell survival was observed. Similarly, murine prostate cancer cell lines containing a Ron deficiency exhibited decreased levels of active NF-kappaB suggesting that Ron may be important in regulating prostate cell survival at least partly through this pathway. In total, our data show for the first time that Ron promotes prostate tumor growth, prostate tumor angiogenesis, and prostate cancer cell survival *in vivo*.

Keywords

Ron receptor; hepatocyte growth factor-like protein; prostate cancer; MST1R; receptor tyrosine kinase

Users may view, print, copy, download and text and data- mine the content in such documents, for the purposes of academic research, subject always to the full Conditions of use: http://www.nature.com/authors/editorial_policies/license.html#terms

*Address correspondence to: Susan E. Waltz, Ph.D., Department of Cancer and Cell Biology, Vontz Building for Molecular Studies, University of Cincinnati College of Medicine, 3125 Eden Ave, Cincinnati, OH 45267-0521, Tel: 513.558.8675, Fax: 513.558.1265, susan.waltz@uc.edu.

Conflict of Interest

The authors declare no conflict of interest.

INTRODUCTION

Prostate cancer remains one of the most commonly diagnosed cancers among men in the United States and is a frequent cause of death from cancer in men. Receptor tyrosine kinases are emerging as potential therapeutic targets in prostate cancer. For example, inhibition of the epidermal growth factor receptor results in decreased prostate cell proliferation (Vicentini et al 2003), and inhibition of the insulin-like growth factor 1 receptor (de Bono et al 2007, Kojima et al 2009) or Her2/neu receptor (Agus et al 1999) reduces tumor growth in mouse prostate cancer cell xenograft models. These data suggest that receptor tyrosine kinases play an important role in prostate tumor growth and should be considered in the development of new treatments in prostate cancer.

One such potential receptor, the Ron receptor, is a member of the Met family of receptor tyrosine kinases. Ron is a heterodimeric glycoprotein consisting of an extracellular alpha-chain and a transmembrane beta-chain (Ronsin et al 1993). Binding of ligand, hepatocyte growth factor-like protein (HGFL), to Ron results in receptor dimerization and phosphorylation on key tyrosine residues within the tyrosine kinase domain (Gaudino et al 1994). Trans-autophosphorylation also occurs on two tyrosine residues within the carboxyl-domain, resulting in the formation of docking sites for adaptor molecules, including PI3-K, PLC-g, Grb2 and Shc. Ron is also upstream of the NF- κ B transcription factor, although the outcome of this regulation is dependent on cell type and context. NF- κ B activity is increased in prostate cancer cells compared to non-transformed prostate cells, and has been shown to be an important regulator of angiogenic chemokine production (Shen and Lentsch 2004).

Based on the numerous pathways activated by Ron, this receptor has been shown to elicit a multitude of biological responses, including cellular proliferation, migration, scattering, survival, and branching morphogenesis (Iwama et al 1996, Meyer et al 2009b, Wagh et al 2008). The Ron receptor tyrosine kinase has also been implicated in the initiation and progression of several human cancers, including those of the breast, colon, skin, and prostate (Chen et al 2000, Maggiora et al 1998, O'Toole et al 2006, Thomas et al 2007). In human prostate cancer cells, Ron is an important regulator of angiogenic chemokine production. Moreover, the regulation of angiogenic chemokines by the Ron receptor has been shown to at least partially be dependent on the NF- κ B transcription factor (Thobe et al 2010). Furthermore, Ron-knockdown PC-3 cells orthotopically transplanted into prostates of nude mice resulted in decreased prostate tumor size and vascularization compared to PC-3 control cells (Thobe et al 2010). While this study suggests the importance of Ron in promoting prostate tumor cell growth *in vivo*, this model does not explain the genetic importance of Ron in the development and progression of prostate cancer.

Mice harboring a deletion of the Ron tyrosine kinase domain, termed Ron TK^{-/-} mice, are overtly normal, although they exhibit alterations in inflammatory responses following stress (Waltz et al 2001). We have previously published in a skin model of chemically-induced carcinogenesis that loss of Ron results in decreased growth of benign skin papillomas, as well as the percent of papillomas that progress to malignancy (Chan et al 2005). In addition, Ron TK^{-/-} mice crossed with mice that are predisposed to develop mammary tumors, display decreased mammary tumor initiation, growth and vascularization (Peace et al 2005).

In order to elucidate the role of the Ron receptor in prostate tumorigenesis *in vivo*, we generated TRAMP mice that are deficient in Ron signaling (TK^{-/-} TRAMP⁺ mice).

TRAMP mice have expression of the simian virus 40 early genes driven by a prostate-specific rat probasin promoter, specifically expressed in the dorsolateral and ventral lobes of the prostate (Greenberg et al 1995). Male TRAMP mice develop prostate hyperplasia as early as 10-weeks of age, and as young as 18-weeks of age can have invasive adenocarcinoma of the prostate. Interestingly, all mice eventually develop metastasis, mainly to the lymph nodes and lungs (Gingrich et al 1996).

Utilizing cell lines derived from TRAMP tumors, it has been shown that inhibition of the receptor tyrosine kinase EGFR, results in decreased cell migration, although there is no impact on cellular proliferation (Kassis et al 1999). Adult TRAMP males treated with Genistein, a phytoestrogen found in soy food known to have tyrosine kinase inhibitory effects, have more well-differentiated prostate tumors compared to control mice (Wang et al 2007). While these data suggest receptor tyrosine kinases are important in prostate tumorigenesis in the TRAMP mouse model, the role of the Ron receptor has not been established. Therefore, in this study we sought to determine the role of Ron in prostate tumor initiation and growth using the TRAMP model.

RESULTS

Wild-type mouse prostates are similar to Ron TK^{-/-} prostates

Prostates taken from 30-week-old wild-type mice (TK^{+/+}) or age-matched TK^{-/-} mice were analyzed by H&E staining to determine if loss of Ron results in any abnormalities in the prostate. No appreciable differences were observed any of the lobes of the prostates of TK^{-/-} mice compared to controls. Representative prostate tissue from TK^{+/+} and TK^{-/-} mice is depicted in Figure 1A for the anterior prostate. Additional pictures are provided in Supplemental Figure S1.

Ron is highly expressed in TRAMP prostate tumors

To determine if similar to human prostate disease (O'Toole et al 2006, Thobe et al 2010), Ron expression is increased in murine prostate tumors, prostates taken from either 30-week-old wild-type (TK^{+/+}) or age-matched TK^{+/+} TRAMP⁺ mice were stained by immunohistochemistry for Ron expression (Figure 1B). Compared with the minimal expression of Ron observed in the TK^{+/+} mouse prostate, TK^{+/+} TRAMP⁺ prostate tumors have significantly elevated levels of Ron. No Ron expression was detected in TK^{-/-} prostates (data not shown) or in prostates from TK^{-/-} TRAMP⁺ mice (Figure 1B). In addition, we analyzed Ron mRNA levels by quantitative real-time PCR and similarly observed increased Ron transcript levels in TK^{+/+} TRAMP⁺ prostates compared to TK^{+/+} prostates (Figure 1C). No detectable levels of Ron mRNA were found in TK^{-/-} prostates or TK^{-/-} TRAMP⁺ prostates (data not shown). Further examination of Ron expression by Western analyses demonstrates elevated Ron protein expression in TK^{+/+} TRAMP⁺ prostates relative to wild-type TK^{+/+} prostates (Figure 1D).

Ron TK^{-/-} TRAMP⁺ mice have decreased genitourinary (GU) complex and prostate tumor size

Thirty-week old TRAMP mice crossed with mice harboring a targeted deletion of the tyrosine kinase (TK) domain of Ron (TK^{-/-} TRAMP⁺) showed a significant reduction in GU complex and prostate size compared to TRAMP mice expressing wild-type Ron (TK^{+/+} TRAMP⁺, Figure 2A, 2B). The average size of TK^{-/-} TRAMP⁺ prostates was 0.3g and the GU complex was 1.3g at 30-weeks of age. TK^{+/+} TRAMP⁺ prostates weighed on average 2.1g and the GU complex weighted 3.6g this same time point. For comparison, prostates and GU weights from TK^{+/+} mice were 0.18 ± 0.012 g and 0.47 ± 0.035 g, respectively, and did not differ significantly from TK^{-/-} mice. As depicted in Figure 2C, TK^{+/+} TRAMP⁺ prostates from 30-week-old mice were composed of poorly-differentiated prostate cancer characterized by anaplastic sheets of cells with irregular nuclei and very little cytoplasm. Normal glands could be observed within the sheets of anaplastic cells along with associated hemorrhagic areas. A spectrum of pathology ranging from prostatic epithelial neoplasia (PIN) to well-differentiated and poorly-differentiated adenocarcinoma with lesions staining sporadically for cytokeratin, E-cadherin, and synapthophysin were observed in the TK^{+/+} TRAMP⁺ prostates at this time point. In addition, the TK^{+/+} TRAMP⁺ mice had large tumors with the tumors encompassing all or a large fraction of the individual prostate lobes. In contrast, the majority of the TK^{-/-} TRAMP⁺ mice had enlarged prostates with the pathology including normal, PIN and well-differentiated adenocarcinoma and contained a defined glandular architecture with the maintenance of an underlying stroma (Figure 2C).

Lungs from these mice were also analyzed for metastasis by histological analysis. Three out of seven (43%) TK^{+/+} TRAMP⁺ lungs had detectable lung metastases as depicted in Figure 2D. None of the five TK^{-/-} TRAMP⁺ lungs examined contained metastases and a section of a typical lung from these mice is depicted in Figure 2D. While the presence of lung metastases is more in the TK^{+/+} TRAMP⁺ mice compared to the TK^{-/-} TRAMP⁺ mice, the data are not significantly different ($P < 0.09$). The lack of significance may be related to the small sample size and warrants further detailed investigation. Interestingly, while Ron has been shown to regulate macrophage activation in acute injury models *in vivo* (Leonis et al 2002, Waltz et al 2001, Wilson et al 2008), we examined the extent of macrophage recruitment in the TK^{+/+} TRAMP⁺ and TK^{-/-} TRAMP⁺ prostates and found no appreciable differences in the number of F4/80 positive cells (Supplemental Figure S2). While the recruitment of F4/80+ cells may be similar between genotypes, this does not preclude differences in macrophage activation as playing a role in the reduced tumor growth observed in the TK^{-/-} TRAMP⁺ prostates.

Murine TRAMP prostates lacking functional Ron display decreased microvessel density

To determine the extent of prostate vascularization, prostates taken from TRAMP mice containing wild-type Ron (TK^{+/+} TRAMP⁺) or prostates taken from TK^{-/-} TRAMP⁺ mice were stained with a CD31-specific antibody. TK^{-/-} TRAMP⁺ prostates exhibited a decrease in the number of vessels per unit area compared to TK^{+/+} TRAMP⁺ prostates (Figure 3A, B). This decrease in microvessel density was correlated with a significant decrease in the levels of VEGF (Figure 3C). Moreover, the levels of the pro-angiogenic

chemokine CXCL2 were also decreased in TK^{-/-} TRAMP⁺ prostates relative to TK^{+/+} TRAMP⁺ prostates (Figure 3D), although these data were not statistically significant.

TRAMP prostate tumors from TK^{-/-} mice have similar rates of cellular proliferation, but decreased cellular survival

Because of the significant difference in tumor size between TK^{+/+} TRAMP⁺ and TK^{-/-} TRAMP⁺ prostate tumors, we sought to determine if there were any differences in cell proliferation or cell death. Interestingly, both TK^{+/+} TRAMP⁺ and TK^{-/-} TRAMP⁺ tumors had similar amount of proliferation as determined by BrdU incorporation and immunohistochemistry (Figure 4A, 4C). Staining with a PCNA antibody showed similar results as those based on BrdU incorporation (Supplemental Figure S2B). There was however, a significant increase in the number of TUNEL-positive cells in the TK^{-/-} TRAMP⁺ tumors, suggesting a survival advantage may exist in the TK^{+/+} TRAMP⁺ prostate cancer cells (Figure 4B and 4C).

Ron activates NF- κ B in prostate cancer

Ron inhibition in prostate cancer cells results in decreased activation of NF- κ B (Thobe et al 2010), and NF- κ B is constitutively active in TRAMP mouse prostate tumors (Shukla et al 2005). To elucidate a potential mechanism by which Ron may be regulating the viability of the TRAMP prostate epithelial cells, we analyzed levels of NF- κ B activity. Figure 5 demonstrates that prostate epithelial cells derived from TK^{-/-} TRAMP⁺ mice have a significant reduction of NF- κ B reporter activity compared with prostate epithelial cells derived from TK^{+/+} TRAMP⁺ mice (Figure 5A). To substantiate decreased NF- κ B transcriptional activity in the TK^{-/-} TRAMP⁺ prostates, nuclear extracts were generated from prostate tissue of 30-week-old TK^{-/-} TRAMP⁺ and TK^{+/+} TRAMP⁺ mice and examined by Western analysis. A representative experiment is depicted in Figure 5B. The TK^{+/+} TRAMP⁺ prostates consistently displayed increased amounts of nuclear NF- κ B relative to TK^{-/-} TRAMP⁺ prostate tissue, further supporting more NF- κ B activity in the prostates of TK^{+/+} TRAMP⁺ mice.

Cells derived from TRAMP prostate tumors lacking functional Ron have decreased viability

The increased number of TUNEL-positive cells in Ron-deficient TRAMP tumors suggests that Ron signaling may provide a survival advantage. To further examine if cells expressing Ron have increased viability *ex vivo*, we isolated prostate tumor cells from 30-week-old TK^{+/+} TRAMP⁺ and TK^{-/-} TRAMP⁺ mice. These epithelial cells were then analyzed for plasma membrane integrity by propidium iodide (PI) staining and for apoptosis by Annexin V staining utilizing flow cytometry. In examining the tumor cells in complete media or under serum deprivation, no appreciable Annexin V staining was observed under our experimental conditions (data not shown). Similarly, although the TK^{-/-} TRAMP⁺ tumors trended towards increased cleaved caspase-3 staining, there was no significant difference compared with TK^{+/+} TRAMP⁺ tumors (Supplemental Figure S3). However, consistent with our TUNEL staining, we did observe a consistent and significant increase in the number of dead cells, which lost plasma membrane integrity and were permeable to PI

staining, in the TK^{-/-} TRAMP⁺ group compared to the TK^{+/+} TRAMP⁺ group. The average number of dead TK^{+/+} TRAMP⁺ cells was 6.6 ± 1.36 while the average number of dead TK^{-/-} TRAMP⁺ cells was 13.7 ± 1.32 (Supplemental Figure S4).

DISCUSSION

An analysis of Ron expression in prostate tissue from either wild-type (TK^{+/+}) or age-matched TRAMP mice (TK^{+/+} TRAMP⁺) showed that the Ron receptor is highly expressed in prostate tumors relative to normal murine prostate tissue. These data are consistent with several reports documenting increased Ron expression in prostate cancer compared with normal prostate tissue (Dhanasekaran et al 2005, Lapointe et al 2007, O'Toole et al 2006, Thobe et al 2010). The overexpression of Ron is an important finding as prior studies have shown that exogenous Ron overexpression is sufficient to induce the formation of both lung and mammary tumors in mice (Chen et al 2002, Zinser et al 2006), and Ron knockdown has been shown to inhibit activation of NF- κ B in prostate cancer cell lines (Thobe et al 2010).

Our data show for the first time that TRAMP mice deficient in Ron receptor signaling have decreased prostate tumor growth. Similar studies from our laboratory have documented that the Ron receptor is necessary for mammary tumor growth in a polyoma virus middle T (pMT) antigen model of breast cancer. pMT mice deficient in functional Ron were shown to have a longer tumor latency, decreased mammary tumor size and decreased metastasis. However, in the pMT mouse model, a significant decrease in cellular proliferation in Ron-deficient pMT tumors compared to Ron-expressing pMT tumors was observed (Peace et al 2005). In contrast, no appreciable differences in cellular proliferation were observed between 30-week-old TK^{-/-} TRAMP⁺ and TK^{+/+} TRAMP⁺ prostate tumors. These differences may reflect the aggressiveness of the respective tumors, with significant tumor burden observed in the pMT-induced mammary tumor model occurring in less than 2 months while the TRAMP model was evaluated at 8 months of age.

While the difference in prostate tumor size in the TK^{+/+} TRAMP⁺ and TK^{-/-} TRAMP⁺ mice did not correlate with differences in tumor cell proliferation, a significant difference in tumor cell viability was observed between groups. Marked increases in the number of TUNEL-positive cells were observed in prostates from TK^{-/-} TRAMP⁺ mice compared to controls, suggesting the novel finding that Ron may be acting as a pro-survival factor in this model. In addition, prostate epithelial cells derived from TK^{-/-} TRAMP⁺ prostates were less viable *ex vivo* than cells derived from TK^{+/+} TRAMP⁺ prostate, supporting Ron as a regulator of cellular survival, although at present the exact mechanism for these differences remains unclear. Moreover, while no changes were observed in macrophage recruitment in the TK^{+/+} TRAMP⁺ and TK^{-/-} TRAMP⁺ prostates at 30-weeks, this does not preclude the involvement of differential macrophage activation in the TK^{-/-} mice as a mechanism that may regulate prostate tumor growth in the TRAMP model. In addition, our studies do not exclude the possibility of the extracellular portion of Ron remaining in the TK^{-/-} mice and acting as a dominant negative or a sink for Ron ligand which may also ultimately impact prostate tumor growth in the TK^{-/-} TRAMP⁺ mice.

The NF- κ B transcription factor has been shown to be constitutively active in TRAMP mouse prostate tumors, and correlates with altered I κ B α expression and IKK activity (Shukla et al 2005). Furthermore, Ron inhibition in prostate cancer cells results in decreased NF- κ B activity and a decrease in pro-angiogenic chemokine production (Thobe et al 2010). We observed that cells derived from TK $^{-/-}$ TRAMP $^{+}$ prostates have decreased levels of active NF- κ B compared to TK $^{+/+}$ TRAMP $^{+}$ derived cells. Further analysis of the activation of NF- κ B in TRAMP prostate specimens demonstrated decreased levels of nuclear NF- κ B in TK $^{-/-}$ TRAMP $^{+}$ prostates relative to TK $^{+/+}$ TRAMP $^{+}$ prostates, suggesting that Ron may be acting as a pro-survival factor through the regulation of this pathway.

TK $^{-/-}$ TRAMP $^{+}$ tumors also demonstrate a reduction in tumor vascularization compared to TK $^{+/+}$ TRAMP $^{+}$ tumors, suggesting that differences in prostate tumor neovascularization may be important for the differences in prostate tumor growth observed in this study. Prostate tumor angiogenesis is important in the TRAMP mouse model as TRAMP mice crossed with mice containing a knockout of the angiogenic chemokine receptor, CXCR2, have decreased prostate tumor growth and time to tumor formation (Shen et al 2006). In addition, TRAMP mice treated with soluble VEGFR-2 demonstrated decreased prostate tumor volume correlating with decreased vasculature (Becker et al 2002). Our previous studies on prostate cancer cell lines showed that all prostate cell lines tested exhibited VEGF expression, although the VEGF levels did not correlate with Ron expression (Thobe et al 2010). In addition, we also showed that a Ron knockdown in DU145 or PC-3 prostate cancer cells did not alter VEGF expression in these cells. A knockdown of Ron in pancreatic cell lines also did not lead to changes in VEGF levels (Logan-Collins et al 2010). However, the latter studies reported that exogenous administration of the Ron ligand in pancreatic cells was able to stimulate VEGF expression at least at one of the time points examined (Logan-Collins et al 2010). These studies suggest that ligand-induced activation of Ron may influence at least temporal VEGF levels but that decreases in the level of Ron in cancer cell lines, as in the case of the knockdown or knockout cells, does not appear to alter VEGF production. Interestingly, however, studies by Logan-Collins and colleagues show increased CD31 microvessel density (MVD) staining in human pancreatic xenographs when Ron was knocked down. In contrast, the studies in the accompanying report and published studies consistently showed a significant decrease in CD31 vessel staining in tumors lacking Ron expression (Peace et al 2005, Thobe et al 2010). In each case however, all tumors containing decreased Ron (prostate or pancreatic) exhibited increases in cell death as indicated by TUNEL staining. Taken together, these data suggest that the effects of Ron signaling on VEGF expression and vascularization are complex and may be influenced possibly by cell type and/or ligand levels and receptor activation. However, a common theme across all findings is the diminished growth of Ron deficient tumors which is associated with increases in TUNEL staining. Finally, while we did observe a decrease in VEGF mRNA expression in TK $^{-/-}$ TRAMP $^{+}$ tumors compared to TK $^{+/+}$ TRAMP $^{+}$ tumors, this model represents a loss of Ron in all cell types. VEGF modulation in this model might be influenced by the loss of Ron expression in other cell types (such as macrophages) or by the interaction of cell types in the tumor microenvironment which contain a loss of Ron.

Our studies support the Ron receptor tyrosine kinase as being an important factor for prostate tumor growth *in vivo*. Further studies are needed to elucidate the potential role of Ron in the growth of prostate cancers, and to determine if advanced prostate cancers upregulate Ron expression in order to bypass androgen-dependence. Our data support the notion that targeting the Ron receptor in prostate cancer has the potential to regulate prostate tumor angiogenesis and prostate cancer survival, and may therefore lead to a reduction in prostate tumor size. While gene deletion studies such as those presented in this report do not necessarily reflect the response of tumors following targeting Ron pharmacologically, our findings provide the first insight into the Ron receptor signaling system as a potential new therapeutic target in prostate cancer.

MATERIALS AND METHODS

Mice

C57Bl/6 Transgenic Adenocarcinoma of the Mouse Prostate mice were purchased from The Jackson Laboratory (Bar Harbor, Maine). Mice containing a germline deletion of the Ron tyrosine kinase domain (TK^{-/-}) have been previously characterized (Waltz et al 2001). TRAMP⁺ mice were crossed with TK^{-/-} mice to generate TK^{+/-} mice with TRAMP. These latter mice were crossed with TK^{+/-} mice to obtain wild-type Ron TRAMP mice (TK^{+/+} TRAMP⁺) and Ron-deficient TRAMP mice (TK^{-/-} TRAMP⁺). Only hemizygous TRAMP males (here-on referred to as TRAMP⁺) were used for experimental analyses. All animals used were in the C57Bl/6 genetic background. The use and maintenance of animals was performed under protocols approved by the Institutional Animals and Use Committee of the University of Cincinnati. For obtaining weight measurements for the genitourinary complex and the prostate, mice were euthanized and the genitourinary complex (consisting of prostate, seminal vesicles, urethra and bladder) was first removed and weighed. If the bladder was full upon dissection, it was punctured to ensure the weight was not including urine. The prostate was then dissected from the genitourinary complex and weighed. Measurements are displayed as weight in grams.

Prostate Histology and Immunohistochemistry

Immunohistochemistry of prostate sections from paraffin embedded 30-week-old wild-type (TK^{+/+}), TK^{-/-}, TK^{+/+} TRAMP⁺ or TK^{-/-} TRAMP⁺ prostates were processed as previously described (Peace et al 2005, Zinser et al 2006). For Ron staining, the Ron C-20 antibody (1:50, Santa Cruz Biotechnology, Santa Cruz, CA) was applied to tissues overnight at 4 degrees. The next day, goat anti-rabbit secondary antibody (Vector Laboratories, Burlingame, CA) was added to the tissues, and following amplification with a VECTASTAIN ABC kit (Vector Laboratories, Burlingame, CA), positive cells were visualized with DAB substrate (Vector Laboratories, Burlingame, CA). The sections were counterstained with hematoxylin, dehydrated, and mounted with permount (Fisher Scientific, Pittsburgh, PA). CD31 staining was performed and quantified as previously described (Thobe et al 2010), and cleaved caspase-3 staining was performed according to the manufacturer's instructions (1:100 Catalog #9664, Cell Signaling Technology, Danvers, MA). F4/80 and PCNA staining was performed as previously described (Mallakin et al 2006, Meyer et al 2009a). For the analysis of proliferation, two hours before sacrifice, 30-

week-old TK^{+/+} TRAMP⁺ or TK^{-/-} TRAMP⁺ mice were injected intraperitoneally with bromodeoxyuridine (BrdU) and sections from paraffin embedded prostate tissue were stained utilizing a BrdU staining kit (Amersham, Piscataway, NJ) according to the manufacturer's instructions. Image J software was used to determine the number of positive cells normalized to area of prostate tissue. For TUNEL analyses, prostate sections from 30-week-old mice were stained using an In Situ Cell Death Detection Kit, AP (Roche Applied Science, Indianapolis, IN) according to the manufacturer's directions, with a 1:2 dilution of TdT enzyme. The number of TUNEL-positive cells was determined by counting as previously described (Peace et al 2005).

Lung Metastasis

For analysis of lung metastases, lungs from 30-week-old TK^{+/+} TRAMP⁺ or TK^{-/-} TRAMP⁺ mice were harvested, fixed in 10% neutral buffered formalin overnight, processed and were paraffin-embedded. 4- μ m sections were cut at 50- μ m intervals, and were examined by hematoxylin and eosin staining for metastases. Mice were counted as positive for lung metastasis if at least one metastatic focus was observed.

Quantitative Real-Time PCR

RNA was isolated from frozen prostate tissue from 30-week-old mice using the Trizol method (Invitrogen, Carlsbad, CA). The High Capacity complementary DNA kit (Applied Biosystems, Foster City, CA, USA) was used to convert RNA to cDNA as per the manufacturer's instructions, and SYBR green incorporation (Applied Biosystems, Foster City, CA) was used to measure gene expression. Primer sequences used were as follows: VEGF_a forward: GCA GAA GTC CCA TGA AGT GA VEGF_a, reverse: TCC AGG GCT TCA TCG TTA; CXCL2 forward: AGTGAAGTGCCTGTCAATGC, reverse: AGGCAAACCTTTTGGACCGCC. Primers for Ron were previously described (Meyer et al 2009b). Gene expression values were normalized to β -glucuronidase (Gus) (forward: TTGAGAACTGGTATAAGACGCATCAG, reverse: TCTGGTACTCCTCACTGAACATGC). Relative gene expression values are shown.

Western Analyses

For total protein analyses, frozen prostate tissues were homogenized in 1 \times Laemmli buffer and were briefly sonicated. Nuclear and cytoplasmic extracts were isolated as previously described (Wagh et al 2011). Protein concentrations were determined using the MicroBCA kit (Pierce Biotechnology, Rockford, IL) according to manufacturer's instructions. 200ug of protein (for Ron) was loaded into a 6% polyacrylamide gel as previously described (Thobe et al 2010). Primary antibodies used were: Ron C-20 (1:200 Santa Cruz Biotechnology, Santa Cruz, CA), anti-total p65 (Cell Signaling, Boston, MA) and Actin (1:40,000 a gift from Dr. James Lessard, Cincinnati Children's Hospital Medical Center, Cincinnati, OH). Membranes were then incubated with a peroxidase-conjugated anti-rabbit or an anti-mouse secondary antibody (Jackson ImmunoResearch Laboratories, West Grove, PA), followed by detection of the antibody with the ECL Plus reagent (Amersham Biosciences, Piscataway, NJ). Protein bands were detected using autoradiography.

Prostate Cell Isolations

Prostate tumor cells were isolated from prostates of 30-week-old mice and placed into 25 ml digestion media containing DMEM/F12, 1 mg/ml collagenase (Worthington Biochemical, Lakewood, NJ), Penicillin/Streptomycin, and 2 mg/ml bovine serum albumin (Sigma, St. Louis, MO) for approximately 2 h at 37°C with shaking at 200 rpm. Cells were then centrifuged for 5 min at 1000 rpm and supernatant removed. To further dissociate epithelial cells, the pellet was resuspended in DMEM/F12 containing 2 U/ml DNase for 5 min with vigorous shaking. DNase was inactivated with equal volume of DMEM/F12 containing 5% FBS. Cells were centrifuged for 5 min at 800 rpm, supernatant was removed and pellet was resuspended in 1× PBS plus 5% FBS. To remove fibroblasts, cells were shaken vigorously then pulse spun for 10 s to a maximum of 1000 rpm, supernatant was removed and spins were repeated 6 additional times. Isolated primary tumor cells were utilized prior to 10 passages and were positive for both cytokeratin expression and androgen receptor status. Purity ranged from 80 to 90%.

NF-κB Analyses

NF-κB reporter assays, on isolated prostate cancer epithelial cells from TK+/+ TRAMP+ and TK-/- TRAMP+ mice, were performed as previously described (Thobe et al 2010). Briefly, 70,000 cells were plated in triplicate in complete media. The next day, cells were transfected using Lipofectamine 2000 (Invitrogen, Carlsbad, CA, USA) with either a NF-κB reporter (pNF-κBluc) or an empty vector (pTAL-luc) construct and a control plasmid expressing Renilla (pRL-TK). At 48hrs after transfection, the cells were lysed and subjected to a dual luciferase assay according to manufacturer's protocol (Promega Corporation, Madison, WI). Results are displayed as relative NF-κB reporter activity where NF-κB luminescence in each sample was normalized to the extent of Renilla expression.

Flow Cytometry

Forty-eight hours after plating cells, media was spun to collect any dead or apoptotic cells not adhered to the dish, and adherent cells were collected by trypsinization. The cell pellets were washed with phosphate buffered saline and binding buffer. Annexin V and Propidium Iodide (PI) were added to the cells according to the manufacturers' instructions (ApoAlert Annexin V-FITC Apoptosis Kit, Clontech, Mountain View, CA). The samples were analyzed using a Coulter Epics XL instrument (Beckman Coulter, Miami, FL).

Statistical Analyses

Data are expressed as mean ± standard error (SE). Student's t-test was used for pair-wise comparisons and Mann-Whitney Rank Sum Tests were applied when applicable using SigmaPlot 11.0 software (Systat Software, Inc., San Jose, CA). Differences between groups were accepted as significant when $p < 0.05$.

Supplementary Material

Refer to Web version on PubMed Central for supplementary material.

Acknowledgements

The authors would like to thank Sandy Schwemberger for her assistance with the flow cytometry experiments as well as Gina Ciovacco for her technical contributions. This work was supported by Public Health Services Grant CA-125379 (S.E.W.) from the National Institutes of Health, and by grant project #PC060821 (M.N.T.) from the Department of Defense Congressionally Directed Medical Research Program.

REFERENCES

- Agus DB, Scher HI, Higgins B, Fox WD, Heller G, Fazzari M, et al. Response of prostate cancer to anti-Her-2/neu antibody in androgen-dependent and -independent human xenograft models. *Cancer Res.* 1999; 59:4761–4764. [PubMed: 10519379]
- Becker CM, Farnebo FA, Iordanescu I, Behonick DJ, Shih MC, Dunning P, et al. Gene therapy of prostate cancer with the soluble vascular endothelial growth factor receptor Flk1. *Cancer biology & therapy.* 2002; 1:548–553. [PubMed: 12496487]
- Chan EL, Peace BE, Collins MH, Toney-Earley K, Waltz SE. Ron tyrosine kinase receptor regulates papilloma growth and malignant conversion in a murine model of skin carcinogenesis. *Oncogene.* 2005; 24:479–488. [PubMed: 15531916]
- Chen YQ, Zhou YQ, Angeloni D, Kurtz AL, Qiang XZ, Wang MH. Overexpression and activation of the RON receptor tyrosine kinase in a panel of human colorectal carcinoma cell lines. *Exp Cell Res.* 2000; 261:229–238. [PubMed: 11082293]
- Chen YQ, Zhou YQ, Fisher JH, Wang MH. Targeted expression of the receptor tyrosine kinase RON in distal lung epithelial cells results in multiple tumor formation: oncogenic potential of RON in vivo. *Oncogene.* 2002; 21:6382–6386. [PubMed: 12214279]
- de Bono JS, Attard G, Adjei A, Pollak MN, Fong PC, Haluska P, et al. Potential applications for circulating tumor cells expressing the insulin-like growth factor-I receptor. *Clin Cancer Res.* 2007; 13:3611–3616. [PubMed: 17575225]
- Dhanasekaran SM, Dash A, Yu J, Maine IP, Laxman B, Tomlins SA, et al. Molecular profiling of human prostate tissues: insights into gene expression patterns of prostate development during puberty. *FASEB J.* 2005; 19:243–245. [PubMed: 15548588]
- Gaudino G, Follenzi A, Naldini L, Collesi C, Santoro M, Gallo KA, et al. RON is a heterodimeric tyrosine kinase receptor activated by the HGF homologue MSP. *The EMBO journal.* 1994; 13:3524–3532. [PubMed: 8062829]
- Gingrich JR, Barrios RJ, Morton RA, Boyce BF, DeMayo FJ, Finegold MJ, et al. Metastatic prostate cancer in a transgenic mouse. *Cancer Res.* 1996; 56:4096–4102. [PubMed: 8797572]
- Greenberg NM, DeMayo F, Finegold MJ, Medina D, Tilley WD, Aspinall JO, et al. Prostate cancer in a transgenic mouse. *Proc Natl Acad Sci U S A.* 1995; 92:3439–3443. [PubMed: 7724580]
- Iwama A, Yamaguchi N, Suda T. STK/RON receptor tyrosine kinase mediates both apoptotic and growth signals via the multifunctional docking site conserved among the HGF receptor family. *Embo J.* 1996; 15:5866–5875. [PubMed: 8918464]
- Kassis J, Moellinger J, Lo H, Greenberg NM, Kim HG, Wells A. A role for phospholipase C-gamma-mediated signaling in tumor cell invasion. *Clin Cancer Res.* 1999; 5:2251–2260. [PubMed: 10473113]
- Kojima S, Inahara M, Suzuki H, Ichikawa T, Furuya Y. Implications of insulin-like growth factor-I for prostate cancer therapies. *Int J Urol.* 2009; 16:161–167. [PubMed: 19183230]
- Lapointe J, Li C, Giacomini CP, Salari K, Huang S, Wang P, et al. Genomic profiling reveals alternative genetic pathways of prostate tumorigenesis. *Cancer research.* 2007; 67:8504–8510. [PubMed: 17875689]
- Leonis MA, Toney-Earley K, Degen SJ, Waltz SE. Deletion of the Ron receptor tyrosine kinase domain in mice provides protection from endotoxin-induced acute liver failure. *Hepatology.* 2002; 36:1053–1060. [PubMed: 12395314]
- Logan-Collins J, Thomas RM, Yu P, Jaquish D, Mose E, French R, et al. Silencing of RON receptor signaling promotes apoptosis and gemcitabine sensitivity in pancreatic cancers. *Cancer Res.* 2010; 70:1130–1140. [PubMed: 20103639]

- Maggiora P, Marchio S, Stella MC, Gai M, Belfiore A, De Bortoli M, et al. Overexpression of the RON gene in human breast carcinoma. *Oncogene*. 1998; 16:2927–2933. [PubMed: 9671413]
- Mallakin A, Kutcher LW, McDowell SA, Kong S, Schuster R, Lentsch AB, et al. Gene expression profiles of Mst1r-deficient mice during nickel-induced acute lung injury. *Am J Respir Cell Mol Biol*. 2006; 34:15–27. [PubMed: 16166746]
- Meyer SE, Waltz SE, Goss KH. The Ron receptor tyrosine kinase is not required for adenoma formation in Apc(Min/+) mice. *Mol Carcinog*. 2009a; 48:995–1004. [PubMed: 19452510]
- Meyer SE, Zinser GM, Stuart WD, Pathrose P, Waltz SE. The Ron receptor tyrosine kinase negatively regulates mammary gland branching morphogenesis. *Dev Biol*. 2009b; 333:173–185. [PubMed: 19576199]
- O'Toole JM, Rabenau KE, Burns K, Lu D, Mangalampalli V, Balderes P, et al. Therapeutic implications of a human neutralizing antibody to the macrophage-stimulating protein receptor tyrosine kinase (RON), a c-MET family member. *Cancer Res*. 2006; 66:9162–9170. [PubMed: 16982759]
- Peace BE, Toney-Earley K, Collins MH, Waltz SE. Ron receptor signaling augments mammary tumor formation and metastasis in a murine model of breast cancer. *Cancer Res*. 2005; 65:1285–1293. [PubMed: 15735014]
- Ronsin C, Muscatelli F, Mattei MG, Breathnach R. A novel putative receptor protein tyrosine kinase of the met family. *Oncogene*. 1993; 8:1195–1202. [PubMed: 8386824]
- Shen H, Lentsch AB. Progressive dysregulation of transcription factors NF-kappa B and STAT1 in prostate cancer cells causes proangiogenic production of CXC chemokines. *Am J Physiol Cell Physiol*. 2004; 286:C840–C847. [PubMed: 14656722]
- Shen H, Schuster R, Lu B, Waltz SE, Lentsch AB. Critical and opposing roles of the chemokine receptors CXCR2 and CXCR3 in prostate tumor growth. *The Prostate*. 2006; 66:1721–1728. [PubMed: 16941672]
- Shukla S, MacLennan GT, Marengo SR, Resnick MI, Gupta S. Constitutive activation of P I3 K-Akt and NF-kappaB during prostate cancer progression in autochthonous transgenic mouse model. *Prostate*. 2005; 64:224–239. [PubMed: 15712212]
- Thobe MN, Gurusamy D, Pathrose P, Waltz SE. The Ron receptor tyrosine kinase positively regulates angiogenic chemokine production in prostate cancer cells. *Oncogene*. 2010; 29:214–226. [PubMed: 19838218]
- Thomas RM, Toney K, Fenoglio-Preiser C, Revelo-Penafiel MP, Hingorani SR, Tuveson DA, et al. The RON receptor tyrosine kinase mediates oncogenic phenotypes in pancreatic cancer cells and is increasingly expressed during pancreatic cancer progression. *Cancer Res*. 2007; 67:6075–6082. [PubMed: 17616662]
- Vicentini C, Festuccia C, Gravina GL, Angelucci A, Marronaro A, Bologna M. Prostate cancer cell proliferation is strongly reduced by the epidermal growth factor receptor tyrosine kinase inhibitor ZD1839 in vitro on human cell lines and primary cultures. *J Cancer Res Clin Oncol*. 2003; 129:165–174. [PubMed: 12712332]
- Wagh PK, Peace BE, Waltz SE. Met-related receptor tyrosine kinase Ron in tumor growth and metastasis. *Adv Cancer Res*. 2008; 100:1–33. [PubMed: 18620091]
- Wagh PK, Gray JK, Zinser GM, Vasiliauskas J, James L, Monga SP, et al. beta-Catenin is required for Ron receptor-induced mammary tumorigenesis. *Oncogene*. 2011
- Waltz SE, Eaton L, Toney-Earley K, Hess KA, Peace BE, Ihlendorf JR, et al. Ron-mediated cytoplasmic signaling is dispensable for viability but is required to limit inflammatory responses. *J Clin Invest*. 2001; 108:567–576. [PubMed: 11518730]
- Wang J, Eltoum IE, Lamartiniere CA. Genistein chemoprevention of prostate cancer in TRAMP mice. *J Carcinog*. 2007; 6:3. [PubMed: 17367528]
- Wilson CB, Ray M, Lutz M, Sharda D, Xu J, Hankey PA. The RON receptor tyrosine kinase regulates IFN-gamma production and responses in innate immunity. *J Immunol*. 2008; 181:2303–2310. [PubMed: 18684919]
- Zinser GM, Leonis MA, Toney K, Pathrose P, Thobe M, Kader SA, et al. Mammary-specific Ron receptor overexpression induces highly metastatic mammary tumors associated with beta-catenin activation. *Cancer Res*. 2006; 66:11967–11974. [PubMed: 17178895]

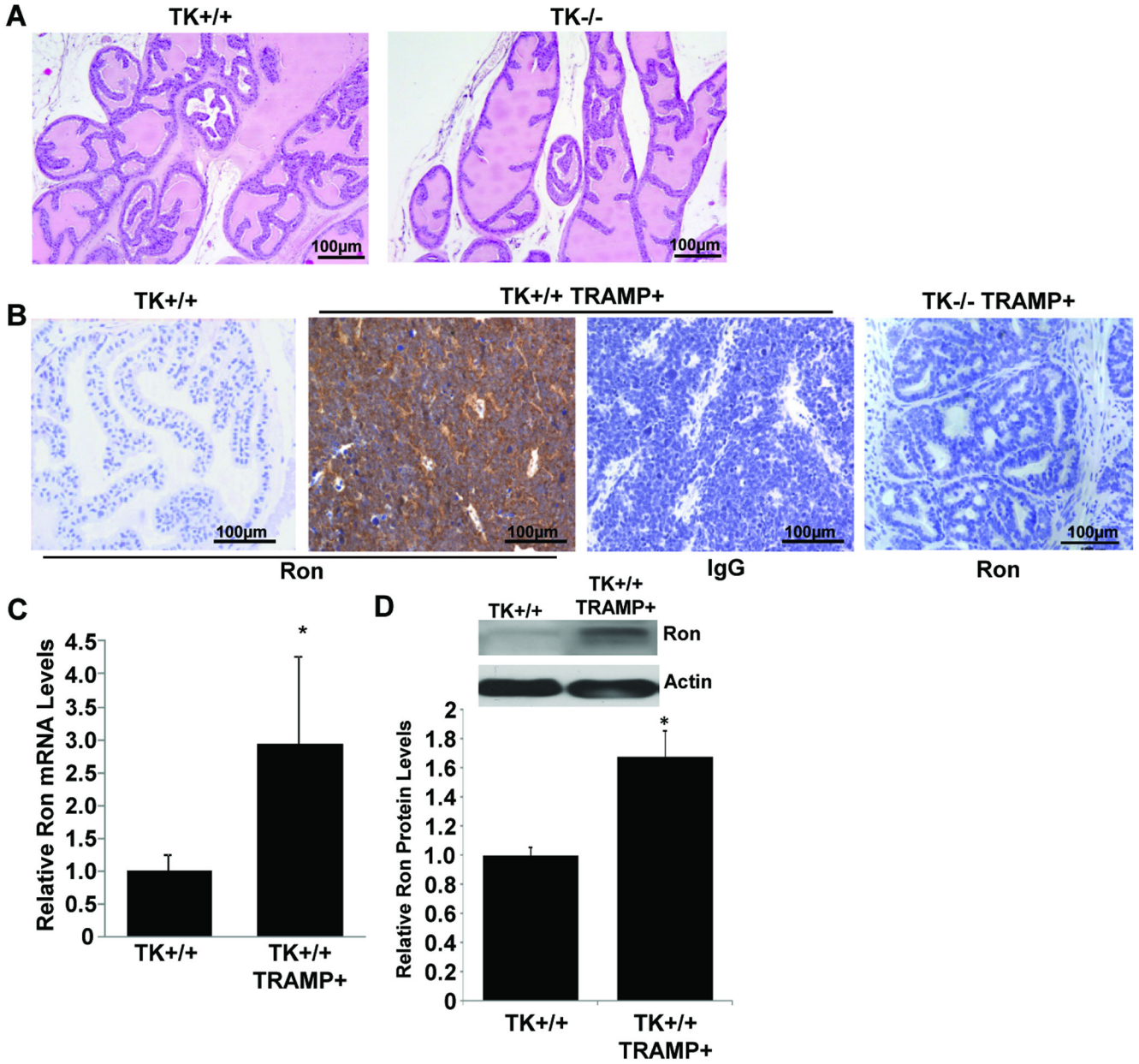


Figure 1. Ron expression in wild-type and TRAMP mouse prostates

A, Prostates from 30-week-old wild-type (TK+/+) or TK-/- mice are histologically similar. Representative sections of the anterior prostates of TK+/+ and TK-/- mice are shown. **B**, Ron is highly expressed in 30-week-old TK+/+ TRAMP+ prostates compared to TK+/+ prostate tissue. No Ron expression is detected in TK-/- TRAMP+ prostates. Representative tissue sections were stained with a Ron-specific antibody or with an isotype control IgG. TK+/+ prostates have minimal Ron expression whereas TK+/+ TRAMP+ prostate tumors have significantly elevated Ron expression. **C**, Quantitative real time PCR analysis demonstrates increased Ron mRNA levels in TK+/+ TRAMP+ prostate tumors (n=5) relative to TK+/+ prostates (n=6). Data are expressed as means ± SE. No detectable Ron mRNA expression

was observed in the prostates of TK^{-/-} or TK^{-/-} TRAMP⁺ mice. **D**, Top: Western analysis of Ron protein levels in a TK^{+/+} prostate and in a prostate tumor from a TK^{+/+} TRAMP⁺ mouse. Bottom: Densitometry analysis of relative Ron protein levels in TK^{+/+} (n=4) and TK^{+/+} TRAMP⁺ (n=5) prostates. Data are expressed as means \pm SE. *p<0.05 compared to TK^{+/+} group.

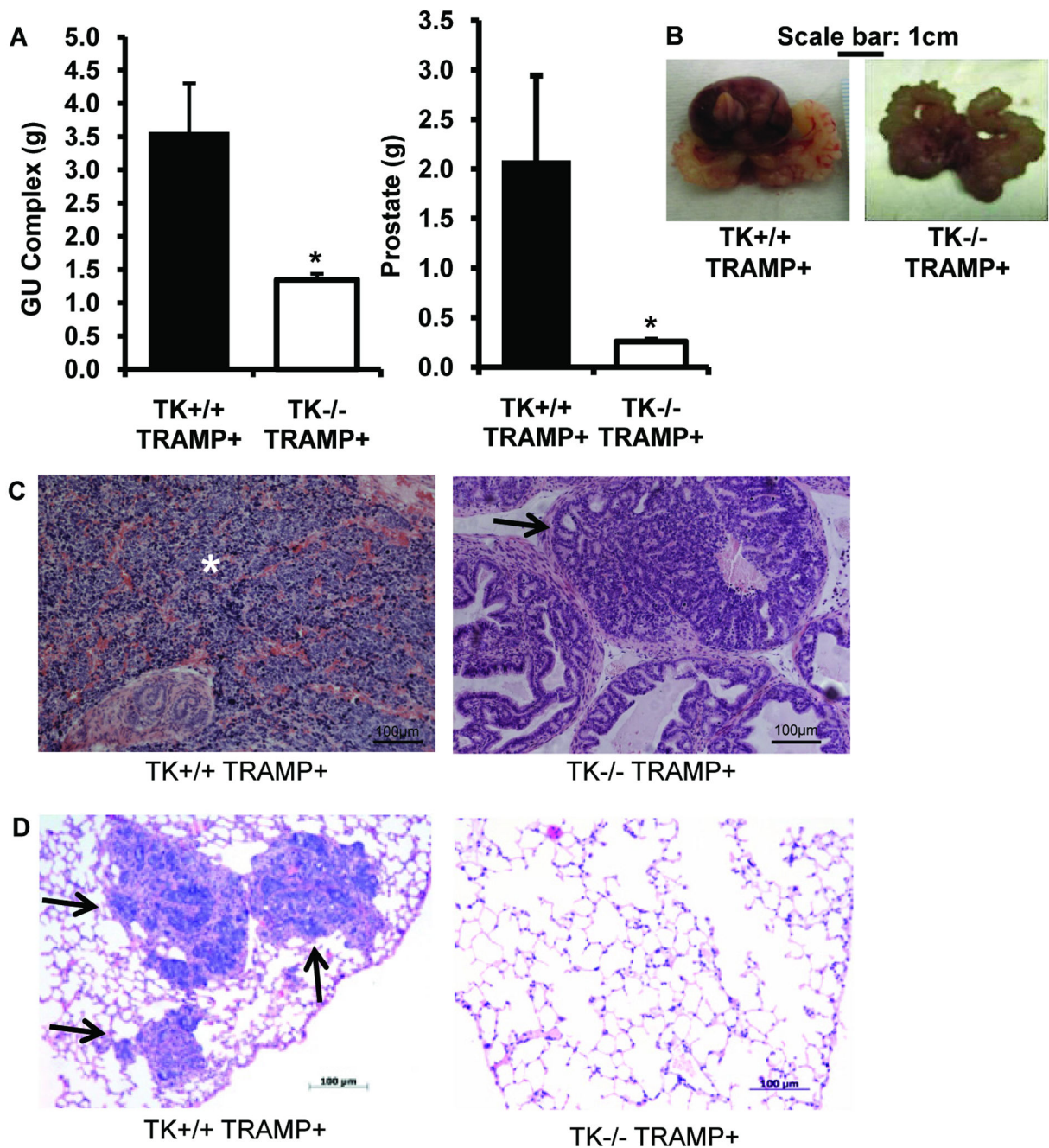


Figure 2. TRAMP mice deficient in functional Ron have decreased genitourinary complex and prostate tumor size

A, 30-week-old TK^{-/-} TRAMP⁺ mice (n=12) exhibit decreased genitourinary (GU) complex and prostate tumor mass relative to TK^{+/+} TRAMP⁺ mice (n=16). Data are expressed as means \pm SE. **B**, Gross examination of genitourinary complexes from TK^{+/+} TRAMP⁺ mice and TK^{-/-} TRAMP⁺ mice demonstrates decreased GU complex size in the TK^{-/-} TRAMP⁺ mice. **C**, Representative histological analysis of TK^{+/+} TRAMP⁺ and TK^{-/-} TRAMP⁺ prostates. The asterisk depicts the large tumor bearing area of the TK^{+/+}

TRAMP+ prostate while the arrow indicates one of the several neoplastic regions of TK^{-/-} TRAMP+ prostate. **D**, Representative image of a lung section containing metastatic foci (arrows) from a TK^{+/+} TRAMP+ mouse and a corresponding section from a TK^{-/-} TRAMP+ lung. Lungs and prostates were stained with hematoxylin and eosin.

Author Manuscript

Author Manuscript

Author Manuscript

Author Manuscript

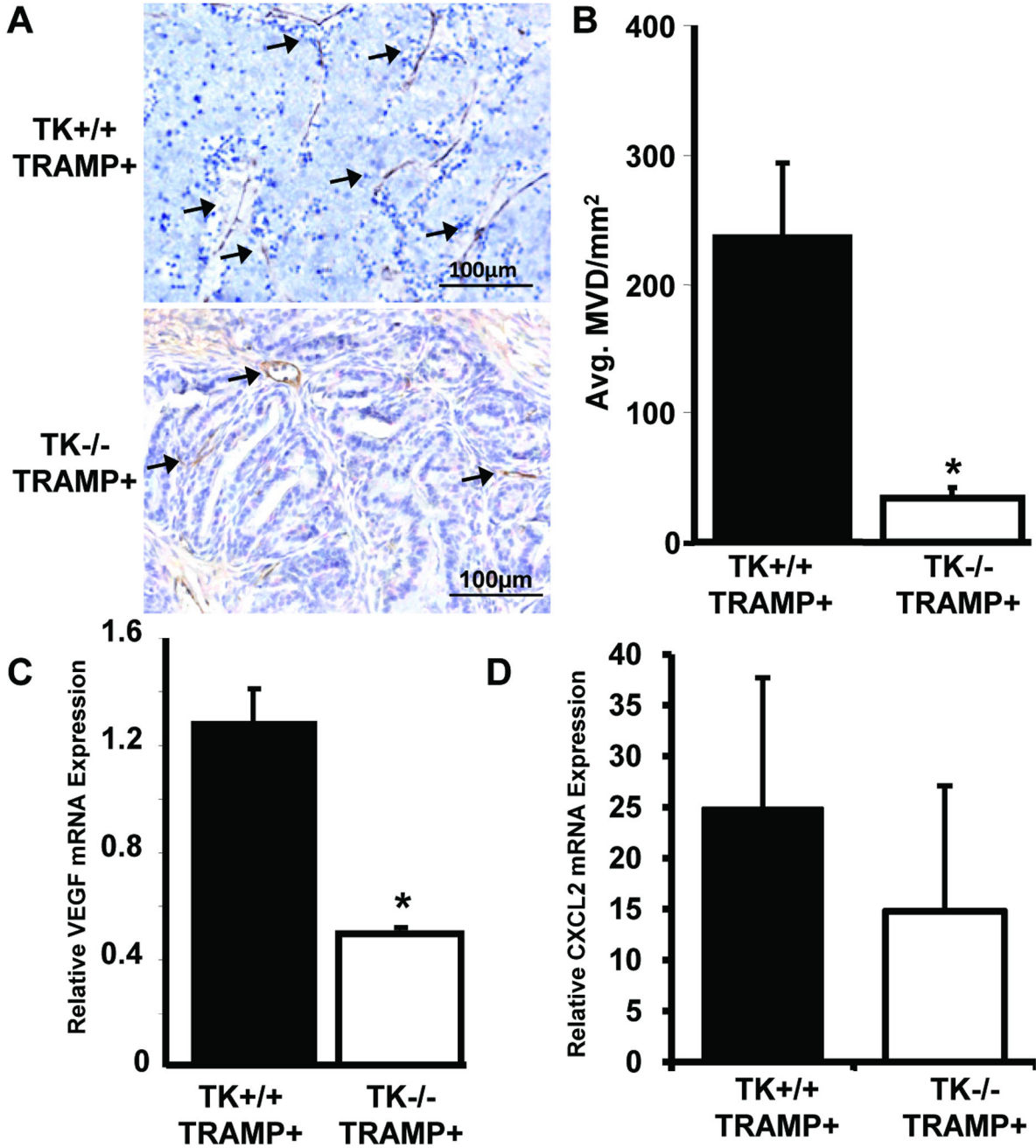


Figure 3. Prostate tumors from TK-/- TRAMP+ mice are less vascularized than prostates from TRAMP mice expressing wild-type Ron

A, TRAMP mice lacking functional Ron (TK-/- TRAMP+) have decreased vascularization as determined by immunohistochemistry with a CD31-specific antibody. **B**, Mean vessel density per area was determined with n=4 mice for the TK+/+ TRAMP+ group and n=3 mice for the TK-/- TRAMP+ group. Data are expressed as means ± SE. *p<0.05 compared to TK+/+ TRAMP+ group. **C&D**, Quantitative real-time PCR was performed on RNA isolated from prostate tumors from TK+/+ TRAMP+ and TK-/- TRAMP+ mice.

Expression of the angiogenic factors VEGF (**C**) and CXCL2 (**D**) are shown. Data are expressed as means \pm SE with n=4 prostates per group. *p<0.05 compared to TK+/+ TRAMP+ group.

Author Manuscript

Author Manuscript

Author Manuscript

Author Manuscript

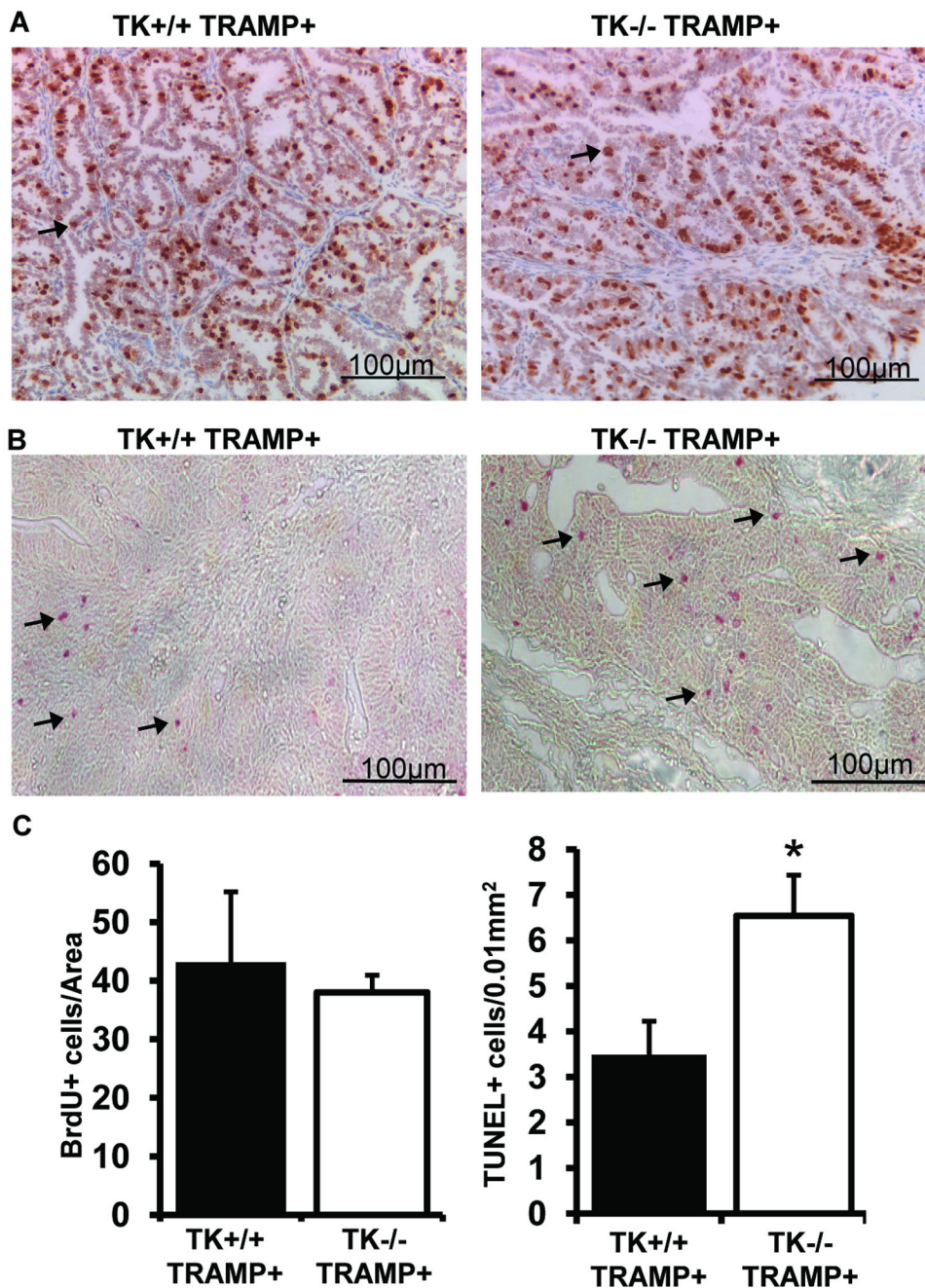


Figure 4. Prostate cell proliferation and apoptosis in TK^{+/+} TRAMP⁺ and TK^{-/-} TRAMP⁺ mice

A, BrdU immunostaining was performed on prostates from 30-week TK^{+/+} TRAMP⁺ and TK^{-/-} TRAMP⁺ mice. **B**, Detection of TUNEL positive cells in prostate tissue of TK^{+/+} TRAMP⁺ and TK^{-/-} TRAMP⁺ mice at 30-weeks of age. **C**, Prostates from 30-week-old TK^{+/+} TRAMP⁺ and TK^{-/-} TRAMP⁺ mice did not exhibit differences in BrdU staining but did contain significant differences in the extent of TUNEL positive cell staining. Data are expressed as means ± SE. Five separate areas were counted from four independent

specimens per group, and representative images are shown. * $p < 0.05$ compared to TK+/+ TRAMP+ group. Arrows depict a few of the positive staining cells.

Author Manuscript

Author Manuscript

Author Manuscript

Author Manuscript

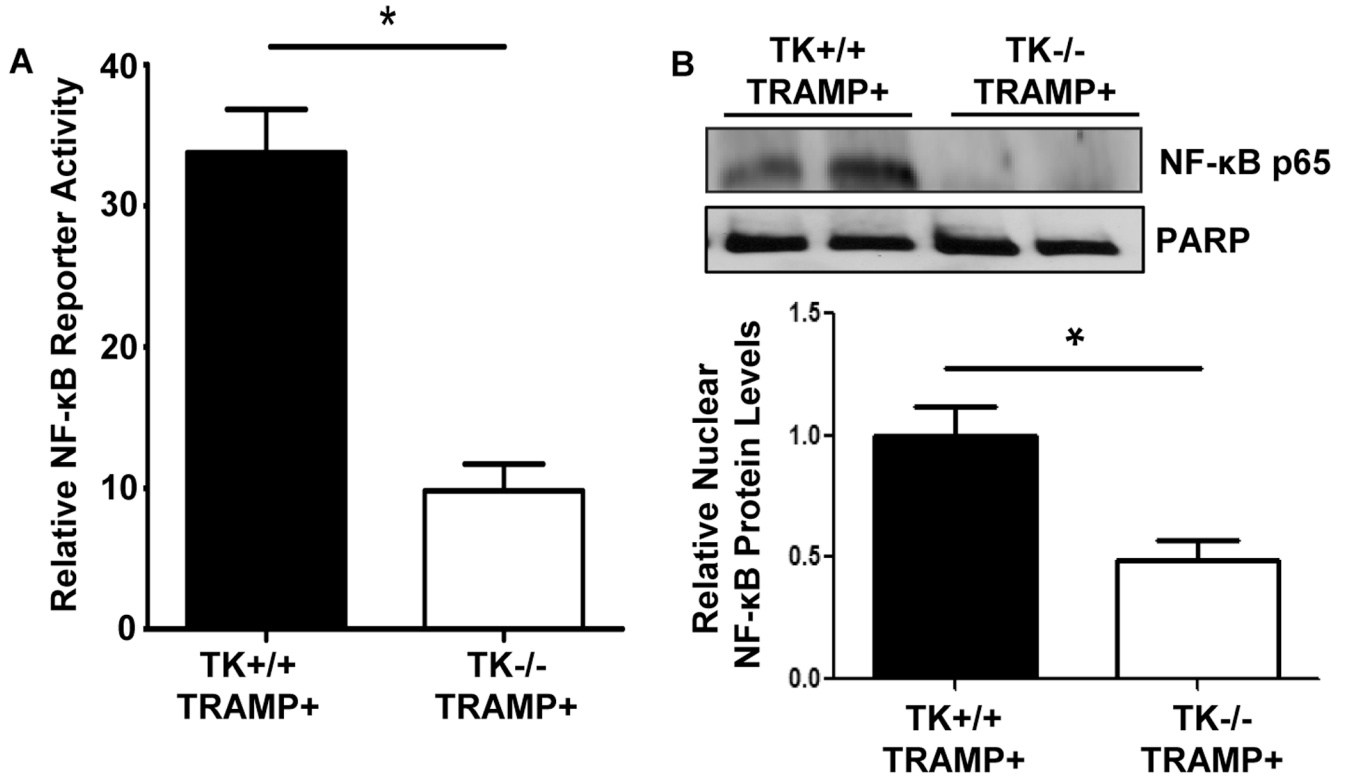


Figure 5. Ron loss in the TRAMP prostate results in decreased levels of active NF-κB
A, NF-κB reporter assays performed with prostate cells derived from TK+/+ TRAMP+ and TK-/- TRAMP+ prostates. Decreased NF-κB reporter activity was observed in TK-/- TRAMP+ cells compared to TK+/+ TRAMP+ cells. Relative NF-κB activity for each sample is depicted. Data are expressed as the mean ± SE. B, Nuclear extracts from 30-week-old TK+/+ TRAMP+ and TK-/- TRAMP+ prostates were isolated and examined by Western analysis. TK-/- TRAMP+ prostates exhibit decreased levels of nuclear NF-κB p65 relative to TK+/+ TRAMP+ prostates. PARP is shown as a nuclear loading control.